

A unified method for the recovery of metals from chalcogenides

*Francesca Bevan,^a Hanaa Galeb,^{a,b} Alexander Black,^a Ioanna Maria Pateli,^{a,c} Jack Allen,^a
Magali Perez,^d Jörg Feldmann,^{d,e} Robert Harris,^a Gawen Jenkin,^f Andrew Abbott,^a
Jennifer Hartley^{a*}*

^a School of Chemistry, University of Leicester, University Road, Leicester, LE1 7RH, UK

^b Department of Chemistry, King Abdulaziz University, 21577 Jeddah, Saudi Arabia

^c Stephenson Institute for Renewable Energy, University of Liverpool, Peach Street, Liverpool, L69 7ZF, UK

^d Department of Chemistry, University of Aberdeen, Meston Walk, Aberdeen, AB24 3UE, UK

^e Institute of Chemistry, University of Graz, Universitätsplatz 1/I, 8010 Graz, Austria

^f School of Geography, Geology and the Environment, University of Leicester, University Road, Leicester, LE1 7RH, UK

E-mail: jmh84@le.ac.uk;

Abstract

Metal chalcogenides are ubiquitous starting materials for the extraction of metals from both primary and secondary sources. In this study, it is shown that chalcogenide compounds are electrochemically active and can be solubilised from solid powders by electrochemical oxidation in a deep eutectic solvent. Importantly, the metal ions released into solution were unaffected by the type of chalcogenide present in the initial compound, maintaining the same speciation as would be obtained from dissolution of a chloride salt. Therefore, metals can be

recovered by the same process from mixtures of chalcogenides. The chalcogenides form a mixture of oxyanions in the +IV and +VI oxidation states, which are separable via standard processes.

Key words

Deep eutectic solvent; chalcogenide; selenium; tellurium; paint casting

Introduction

Metals are commonly found as chalcogenide compounds in the environment, and synthetic oxides, sulfides, selenides and tellurides are used in applications such as semiconductors, solar cells, energy storage, sensors, glass manufacturing, pigments, corrosion resistance, and as additives to improve machining characteristics.¹⁻² The rarer chalcogenides, selenium and tellurium, are usually obtained as by-products from anode slimes generated from the electrolytic copper,³ silver, and gold refining processes.⁴⁻⁵ In pyrometallurgical processing, the chalcogenides are often lost as volatile species during the roasting or leaching stage.⁶⁻⁷ The availability of these elements is hence driven by demand for production of the metal component, rather than demand for the elements themselves.⁸ In recent years, the demand for these elements has increased due to the production of semiconductor materials such as CdTe and copper-indium-gallium-selenide materials.^{6, 9} Tellurium is also being explored as an alternative to current Li ion battery technologies.¹⁰⁻¹¹

Current methods for recovering selenium and tellurium from anode slimes often involve a pyrometallurgical pre-treatment of a soda roast, followed by leaching of the selenium species with either an acid or alkali leach.¹² High purity selenium is then obtained from these solutions by treatment with sulfur dioxide. Alternatively, an oxidative roast of the anode slime can be

used, forming SeO_2 gas which is then trapped and dissolved in water, before precipitation of elemental selenium with sulfur dioxide.¹³ The recovery process for tellurium after removal of the selenium content involves a series of leaching, precipitation and redissolution steps, before finally being electrowon from solution.^{3-4, 12}

Due to increased demand coupled with restricted availability, alternative and milder routes for the processing of metal chalcogenide minerals, or indeed the reprocessing of scrap metal chalcogenide products such as semiconductors, are therefore important. In the present work, we focus on the use of deep eutectic solvents (DESs) to electrochemically leach and recover selenium and tellurium from various metal compounds. DESs are a type of solvent formed from eutectic mixtures of a quaternary salt and hydrogen bond donor (HBD).¹⁴ These solvents have low volatility, high thermal and chemical stability, with a relatively wide potential window, and have the ability to be tailored to specific purposes through judicious choice of both quaternary ammonium salt and HBD.¹⁵⁻¹⁶ Similarly to ionic liquids (ILs) and molten salts, DESs have the advantage of circumventing aqueous/oxide-hydroxide chemistry, and can enable metal speciation and redox behaviour that may otherwise be difficult in aqueous media, e.g. Au can be oxidised with iodine.¹⁷⁻¹⁸ Selenium electrochemistry in DES is especially different to aqueous media¹⁹ and it is therefore likely that the electrochemistry of tellurium may also be equally complex, with the added possibility of chloride species forming.

Choline chloride-based DESs have been previously applied to the electrodeposition of metal chalcogenide thermoelectric or semiconductor films via electrochemical reduction from solutions containing a mixture of the two elements. For example, bismuth telluride films were produced by Agapescu et al.²⁰ and Golgovici et al.²¹ using DESs formed with oxalic acid or malonic acid, respectively. Other DESs made with either ethylene glycol or urea as the HBD

component have been used to deposit films of lead selenide,²² lead telluride,²³ copper telluride²⁴ and zinc telluride.²⁵ During anodic dissolution, it has been shown that oxidation of metal sulfides can lead to simple recovery of metals such as Pb, Fe and Cu,²⁶⁻²⁸ and this has recently been extended to oxides.²⁹

The purpose of the current study is to extend our understanding of chalcogenide behaviour to include selenium and tellurium. In the present work, we aim to investigate the anodic dissolution behaviour of a series of metal chalcogenide compounds in a choline chloride-ethylene glycol DES, with a goal to recover the elements selectively. A preliminary electrochemical series has already been established for selected metals in this DES,³⁰ and we aim to extend it to the chalcogenide species observed here. Finally, we aim to identify (or predict) the final species formed by the metal cation and the oxidised chalcogenide moiety. These data will then be applied to developing the bulk anodic dissolution and recovery of the individual elements from solution.

Experimental

The DES used was made from heating and stirring a 1:2 molar ratio mixture of choline chloride (ChCl, 98% Sigma-Aldrich) and ethylene glycol (EG, 98% Sigma-Aldrich) together at 80 °C until a homogenous liquid formed, as described in the literature.³¹⁻³² All chemicals used for cyclic voltammetry, bulk dissolution and UV-Vis spectroscopy are listed in **Table S1** in the Supporting Information. The balance used was a Mettler Toledo ME analytical balance, with 4 decimal place precision.

For paint casting experiments, the working electrode was a platinum flag working electrode (area ca. 1.5 x 1.5 cm²) bent at an angle of 90° that had been painted with a slurry of ca. 40 mg

of material which had been ground to a paste with DES.²⁸ For the semiconductor materials it was important to ensure that the particle size was as small as possible and only the minimum amount of paste necessary was used on the working electrode, otherwise the resistive current was high and resolution of the redox peaks was poor. Cyclic voltammetry (CV) was performed using an IVIUMnSTAT multichannel potentiostat/galvanostat together with the corresponding Ivium software. The other electrodes were a platinum flag counter electrode, and a 0.1 mol dm⁻³ Ag/AgCl in 1ChCl:2EG reference electrode. The paint casted CVs were started from open circuit potential (OCP), with measurements made for scans in both initial cathodic and anodic directions. All CVs were measured at a scan rate of 10 mV s⁻¹. Formal electrode potentials were determined by taking an average of the oxidation and reduction potentials and referencing them to the [Fe(CN)₆]^{3-/4-} couple.^{30, 33} In cases where a large reduction overpotential was present, a zero current potential on the anodic sweep was taken instead to obtain a rough estimate of the electrode potential. Chronocoulometry measurements were carried out using the same electrode set-up as for CVs, and with a potential of 1.2 V applied to the electrode for 1800 s.

Bulk electrodisolution and electrowinning of the metal chalcogenides was carried out at 1.5 V for 24 hours at room temperature, using a benchtop power supply, with an iridium oxide-coated titanium mesh as the anode in a cell similar to that previously described.²⁷ For bulk dissolution, a second iridium oxide-coated titanium mesh was used as the cathode. For electrowinning, a nickel plate (ca. 4 cm² exposed to solution) was used as the cathode. A slurry was made by grinding the metal chalcogenide together with a small amount of DES, which was then filled into the anode sample chamber, resulting in a sample area exposed to solution of ca. 4 cm². UV-vis measurements of these solutions were then recorded using an UV5Bio (Mettler Toledo) UV-Vis spectrometer between 190 and 1000 nm, with cuvette thickness determined

based on concentration. High performance liquid chromatography (HPLC) measurements were carried out at the University of Aberdeen, using a 1100 Agilent HPLC coupled to an Agilent Technology ICP-MS 7900. The column was a Hamilton PRPX 100, and the internal standard was 10 ng L⁻¹ ⁸⁹Y. The isotopes monitored (dwell time) were: ⁷⁷Se (0.1s), ⁷⁸Se (0.1s), ¹²⁵Te (0.1s), ¹²⁶Te (0.1s), ⁸⁹Y (0.1s). The DES samples obtained from bulk electrodisolution were diluted in milli-Q water, and the buffer solutions were 10 mM ammonium citrate, 2% methanol, pH = 7 (selenium) or 10 mM ammonium phosphate, pH = 10 (tellurium). Standard solutions for calibration were prepared from sodium selenate (SeO₄²⁻, Se^{+VI}), sodium selenite (SeO₃²⁻, Se^{+IV}), sodium tellurite (TeO₃²⁻, Te^{+IV}) and sodium tellurate (TeO₄²⁻, Te^{+VI}). A Hitachi S-3600N Environmental Scanning Electron Microscope (SEM) with Oxford INCA 350 energy-dispersive X-ray spectroscopy (EDX) software was used to analyse the electrowon material for elemental composition.

Results and discussion

Lead chalcogenides as model systems

From previous work,²⁶⁻²⁷ it was seen that anodic dissolution of metal sulfide minerals proceeded via oxidation of the chalcogenide, with high oxidation states seen for the resulting sulfur species. Oxidation of metal oxides led to the suspected formation of superoxide which enabled the metal to be solubilised.²⁹ Here, we investigate the electrochemical behaviour of selenide and telluride, using Pb-chalcogenide compounds as model systems. The advantages of using lead are that Pb^{II} is unlikely to be oxidised further to the unstable Pb^{IV} within the potential window of ChCl:2EG, the redox potential of the Pb^{II/0} couple is likely to be sufficiently cathodic to the oxidation of the chalcogenide species, and the electrochemical behaviour of lead is well-characterised.²⁸ To differentiate the redox processes associated with the chalcogenides from that of lead alone, CVs of the lead-free chalcogenide compounds were

also measured (Na_2S , Na_2Se , and Na_2Te), along with a chalcogenide-free Pb^{II} compound (PbCl_2). The oxidation of chloride would take place alongside the anodic decomposition of the solvent and is not observed within the electrochemical window of the DES.

The paint casted CVs of PbO , PbS , PbSe and PbTe on a Pt-flag electrode in $\text{ChCl}:\text{2EG}$ are shown in **Figure 1**, overlaid with paint casted films of PbCl_2 and the corresponding sodium chalcogenide compounds. From the CV of PbCl_2 , the redox couple for $\text{Pb}^{\text{II}/0}$ can be identified at -0.55 V, followed by the oxidation of a Pb-Pt alloy at ca. -0.30 V.^{28, 34-35} A small cathodic process at ca. -0.2 V can be assigned to underpotential deposition of lead. All other redox potentials can therefore be assumed as related to the chalcogenide species present.

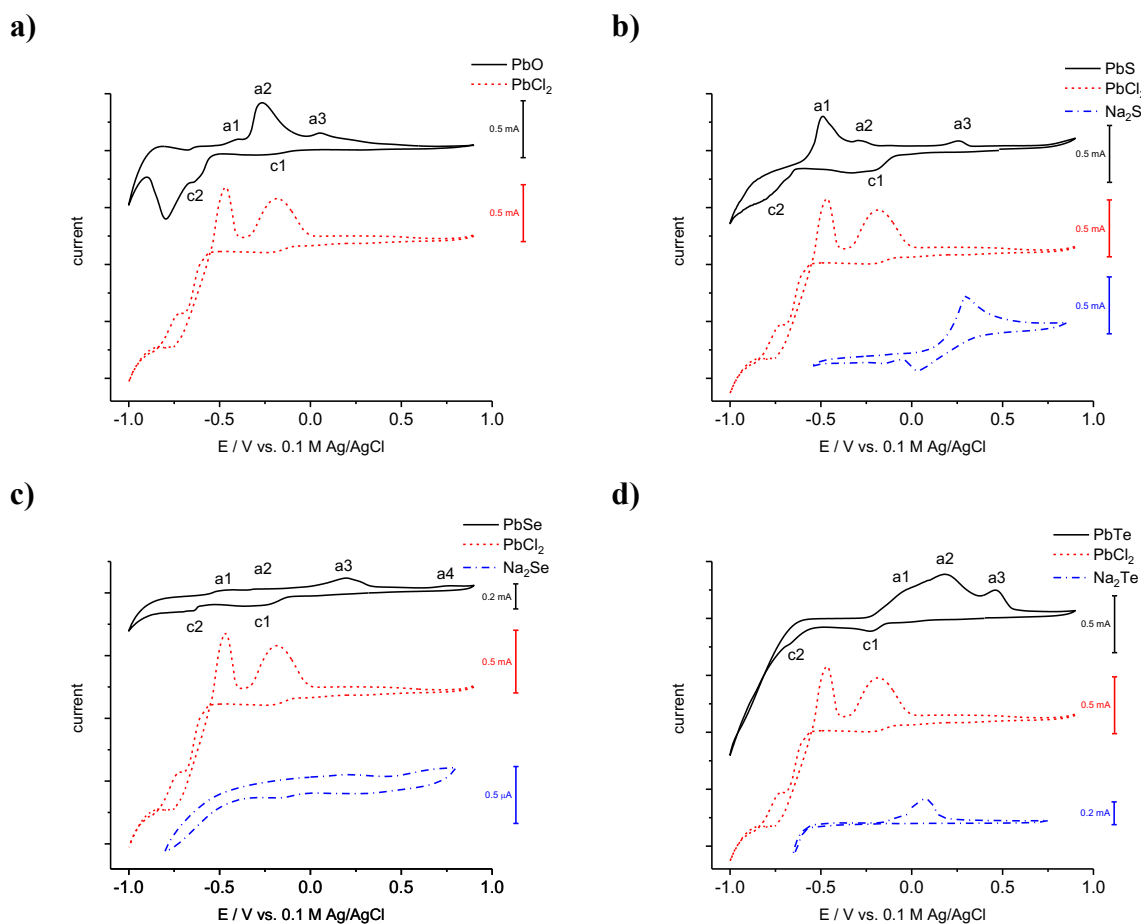


Figure 1. Paint casted CVs of a) PbO, b) PbS, c) PbSe and d) PbTe powders on a Pt flag working electrode in ChCl:2EG, referenced to 0.1 M Ag/AgCl reference electrode. All scans measured at 10 mV s⁻¹. Peak labels correspond to the Pb-chalcogenide CVs.

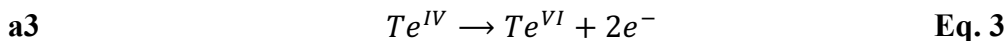
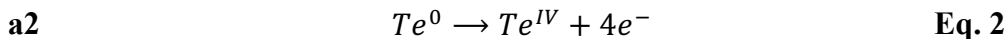
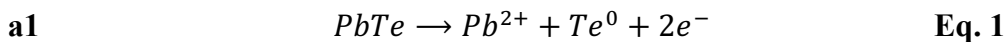
The CV of PbO shows two reduction peaks (**c1**, **c2**) and a series of oxidation peaks (**a1-a3**), which can be assigned to: **c1** underpotential deposition of Pb, **c2** bulk deposition of Pb, **a1** oxidation of Pb, and **a2** oxidation of a Pb-Pt alloy. The smaller current associated with **a1** in the CV of PbO when compared to PbCl₂ is due to different amounts of lead being reduced onto the different electrode surfaces. However, the anodic peak **a3** at ca. +0.06 V is not present on the PbCl₂ scan. A redox process at similar potentials has also been observed during the paint casting of other metal oxides, and has been identified as potentially being oxidation of oxide to the superoxide.²⁹

The PbS system was used as the initial demonstration for the paint casting technique.²⁸ The same Pb-related redox processes are observed in the voltammetry as for PbCl₂. In this system, there is an additional process **a3** (at ca. +0.25 V) that is only observed during the first scan. Comparison to the CV of Na₂S, shows that this can be attributed to the oxidation of S²⁻ to elemental sulfur or sulfate,²⁶ which then forms a passivation layer towards further oxidation of sulfide. The formation of elemental sulfur is known to be a dominant sulfidic reaction product in aqueous electrolytic processes, producing similar problematic effects.³⁶⁻³⁷ The presence of chloride is known to help mitigate formation of passivating sulphur or polysulfide layers in aqueous systems,³⁸⁻³⁹ but does not completely prevent them from forming. In a DES the high chloride concentration not only enables bulk dissolution of PbS but also enables recovery of pure Pb on the cell cathode, as was observed for PbO.²⁹

Applying the paint casting technique to PbSe yields a poorly resolved voltammogram on the first sweep, for both selenium- and lead-related couples. On subsequent scans, the $\text{Pb}^{\text{II}/0}$ couple at **a1/c2** increases in current as more of the higher conducting lead nuclei remain on the surface. After repeated cycling of the paint casted films, an (electro)chemically resistant grey layer was present on the Pt flag electrode (**Figure S1** in the Supporting Information) and linear sweep anodic etching of this film showed oxidation around +0.6 V, a similar potential to that of **a4** in the CV of PbSe. This film is likely to be the grey allotrope of selenium. Therefore, by comparing this CV to that of Na_2Se and to literature data of selenium deposits in $\text{CHCl}_3:\text{2EG}$,²² the anodic process **a3** can be assigned to oxidation of $\text{Se}^{\text{II}-}$ to Se^0 . During further scans, where elemental selenium is present at the electrode surface, the products of its reduction must be accounted for. From these CV data alone, it is unknown whether H_2Se , HSe^- or ‘free’ $\text{Se}^{\text{II}-}$ is generated in solution. However, a good estimate can be made based on aqueous standard potentials for oxidation of these species to elemental selenium ($\text{Se}^0/\text{H}_2\text{Se} = -0.400 \text{ V}$, $\text{Se}^0/\text{HSe}^- = -0.510 \text{ V}$, $\text{Se}^0/\text{Se}^{\text{II}-} = -0.920 \text{ V}$).⁴⁰ Coupled with a characteristic smell generated during cycling, the most likely redox couple is that of $\text{Se}^0/\text{H}_2\text{Se}$.

A more complex case is that of PbTe; on the first sweep, two cathodic processes (**c1** and **c2**) are present, both of which are present for the other Pb-chalcogenide compounds, i.e. reduction of Pb^{II} to Pb metal. However, none of the three anodic processes (**a1-a3**) are at potentials where oxidation of elemental lead is expected to take place, based on the behaviour of the other lead compounds. Given the more metallic character of Te compared to the other chalcogenides, a PbTe alloy may form at the electrode surface,^{23, 41} making an assignment of **a1** to oxidation of that alloy reasonable. Processes **a2** and **a3** are likely to be related to oxidation of tellurium species. The exact speciation of these tellurium complexes are unknown, however it is likely that the ions form O-coordinated complexes, as will be discussed later. Assuming that the E-

pH diagram of Pb-Te-H₂O systems are a valid tool to predict behaviour in DES media, the dissolution electrochemistry could potentially be assigned to the following equations:



However, a complicating factor is for process **a3** being assigned to the Te^{VI/IV} couple is that it does not appear in the Na₂Te system. It also does not appear in the PbCl₂ system, so it is unlikely to be the Pb^{IV/II} couple. In this particular instance, processes **a2** and **a3** might be part of the same oxidation process, but with the formation of a passivating layer of TeO₂, as in aqueous systems oxidation to form the Te^{IV} solution species is thermodynamically unfavourable.^{40, 42} Processes **c1** and **c2** are once again likely related to reduction of Pb^{II} to Pb⁰.

Other chalcogenide systems & formal redox potentials

The electrochemical behaviour of a series of metal chalcogenide compounds are shown in **Figure 2**. The dashed lines represent where the electrode potentials should be for the metal oxidation and reduction couples in isolation from the chalcogenides.³⁰ From these two graphs, it can be seen that the more chlorophilic metals, copper, silver, and bismuth, are unaffected by the presence of chalcogenide during the recording of CVs. For lead and zinc, which are known to retain similar formal electrode potentials in both DES and aqueous media, the electrochemistry is more greatly influenced by the presence of the chalcogenide.

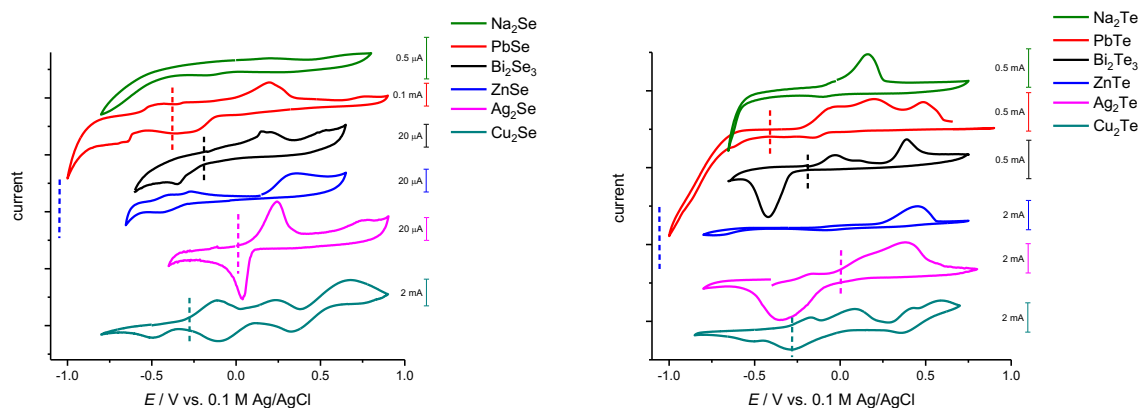


Figure 2. Paint casted CVs of different selenide (left) and telluride (right) compounds on a Pt flag working electrode in ChCl:2EG, referenced to 0.1 M Ag/AgCl reference electrode. All scans measured at 10 mV s^{-1} . Dashed lines represent formal oxidation potentials for the non-chalcogenide elements present.

Speciation of dissolved elements in electrolysis solutions

The speciation of the metal ions in the solutions produced from anodic dissolution of chalcogenide compounds in ChCl:2EG was determined using UV-vis spectroscopy, with the spectra shown in **Figure 3**. It can be seen that the type of chalcogenide present has minimal effect on the speciation of the metal cation, and that the metal cations retain the same speciation in solution as that obtained from the dissolution of the corresponding chloride salts, i.e. forming the expected $[\text{MCl}_2]^-$ and $[\text{MCl}_4]^{x-}$ complexes.⁴³ This shows that the anodic oxidation only involves the chalcogenide moiety and does not change the metal oxidation state. Only in the case of copper, where two oxidation states are easily accessible within the potential window of the solvent, does a variation in speciation appear, i.e. the solution produced from Cu_2S forms Cu^{II} species in solution, whereas Cu^{I} species are present in the solutions of Cu_2Se and Cu_2Te . It is not clear whether this effect is linked to the chalcogenide, or to the lower stability of the Cu^{I} state in DES and its potential to be oxidised further by the presence of dissolved oxygen in the DES.

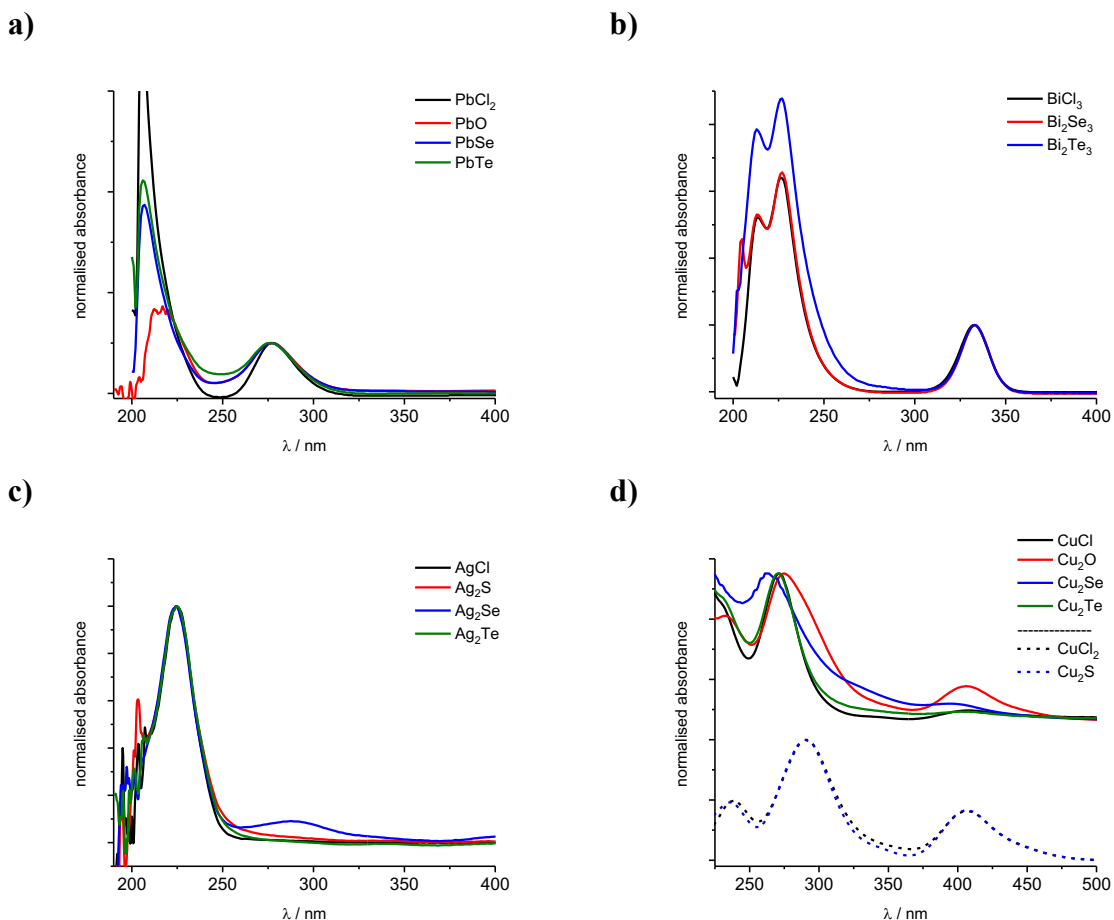


Figure 3. Normalised UV-vis spectra of electrodissolved metal chalcogenides in ChCl:2EG, where the metal is: a) lead, b) bismuth, c) silver, and d) copper. Reference solutions made from chemical dissolution of the relevant chloride salt. Note the two references for copper, as two oxidation states are accessible in the DES.

For the chalcogenide species, UV-vis is a less useful technique as the anticipated species are unlikely to have chromophores. Whilst not directly comparable to DES media, aqueous Pourbaix diagrams can be used as an indication of which species might be present under the particular potential and pH conditions employed. In oxidising regimes with a pH of 7 (the approximate pH of ChCl:2EG),⁴⁴ the chalcogenide species most likely to be present will therefore be SO_4^{2-} , SeO_3^{2-} , SeO_4^{2-} , HTeO_3^- and HTeO_4^- .⁴⁰ Oxidation of oxide, on the other hand, is thought to proceed via a superoxide intermediate in DES media.²⁹ HPLC

measurements carried out on solutions of copper(I) selenide and copper(I) telluride show that selenium and tellurium are present as a combination of selenite/selenate and tellurite/tellurate species, most likely coordinated to oxygen-donor ligands (see **Figure 4**).

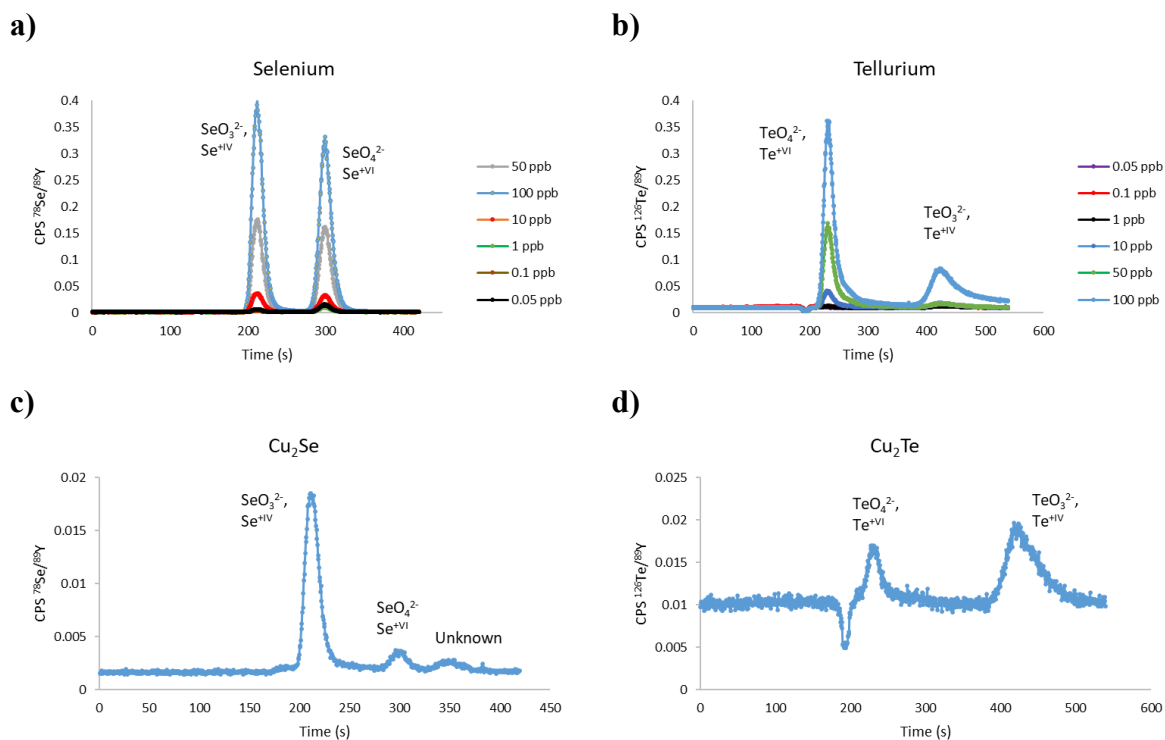


Figure 4. HPLC traces showing the selenium and tellurium species detected in the standard solutions (a & b), and in solutions of anodically dissolved c) Cu_2Se and d) Cu_2Te in $\text{ChCl}:\text{2EG}$.

Although the exact coordinating ligands in the chalcogenide species remain unknown, from these data it can reasonably be assumed that the metal remains free from chalcogenide coordination in solution. These coordinating ligands could be identified via X-ray absorption techniques, such as extended X-ray absorption fine structure (EXAFS) spectroscopy, which permits identification of coordinating atom type and number, and chalcogenide-ligand path lengths. This has the implication that any electrowinning/cementation processes for recovery of specific metals from a mixed element solution should proceed by similar rates and mechanisms, no matter the chalcogenide present in the starting compound. Recovery of

selenium and tellurium may however prove more challenging, as they are anticipated to form very stable high oxidation state O-coordinated complexes.

Recovery of the metals and chalcogenides

The electrowinning of copper was carried out from the different copper chalcogenide systems, as it has previously been demonstrated that copper could be recovered from anodic dissolution solutions of copper sulphides.²⁶ The sulfur was determined to be present in solution in the form of sulfate, as determined by the aqueous BaCl₂ spot test. Copper could also be directly recovered during anodic dissolution of copper oxide at the cathode of iridium oxide-coated Ti mesh.²⁹ In the present work, nickel plates were used as cathodes in solutions of bulk dissolved CuS, Cu₂S, Cu₂Se, CuSe, Cu₂Te, the colours of which and electrodeposits are shown in **Figure 5**. For all cases, copper is electrowon regardless of the initial oxidation state of the copper or the type of chalcogenide present, presenting a universal method of recovery from a range of starting materials. The EDX values for each of the copper coatings are shown as a Cu:O ratio, and a high copper purity was obtained. There were no traces of S, Se or Te in the respective deposits, which is in agreement with the speciation data that indicated the chalcogenide is present in solution as a stable species with a high oxidation state. To recover the chalcogenides in their elemental states would require an inefficient 6 or 8 electron process, along with a substantial applied potential to overcome the generation of any solid oxides. This approach can also be carried out for other metals.⁴⁵

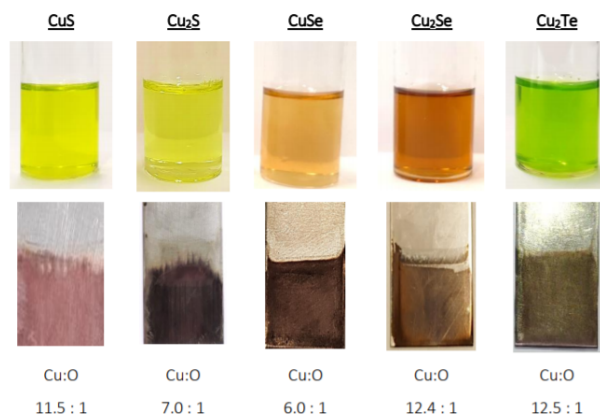


Figure 5. Solutions obtained after electrochemical dissolution of: CuS, Cu₂S, CuSe, Cu₂Se and Cu₂Te (top), and the corresponding electrodeposits (bottom). The Cu:O ratios were obtained from EDX measurements.

Chalcogenides can be detected in aqueous systems by various chemical means, including via the addition of hydrazine, thiourea, hydriodic acid, acidic iron(II) sulfate solution, or aqueous BaCl₂ solution.⁴⁶ In this work the iron(II) sulfate with phosphoric acid test was employed, as it results in the formation of the same elemental chalcogenide precipitates in DES media as it does in aqueous media. The results of these tests can be seen for Ag₂Se/Ag₂Te and ZnSe/ZnTe in **Figure 6**. These were selected because of the colourless nature of the metal chloride complexes [AgCl₂]⁻ and [ZnCl₄]²⁻, which allows the results of the precipitation test to be seen more clearly. For both telluride systems, a black precipitate of elemental tellurium formed. A positive result for selenium was only observed for the ZnSe solution with the precipitation of the red allotrope of selenium. No precipitate was observed from the Ag₂Se solution, but this may be due to a much lower concentration of selenium ions in solution. EDX analysis confirmed the presence of Se or Te in the precipitates.

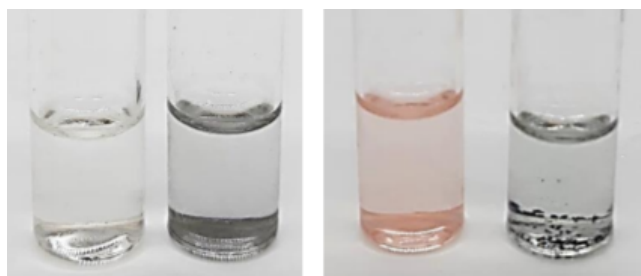


Figure 6. Spot test results for detecting selenium and tellurium in solutions obtained by electrochemical dissolution at 1.5 V for 24 hours in $\text{CHCl}_3\text{:}2\text{EG}$, using the iron sulfate in phosphoric acid test. Left: Ag_2Se & Ag_2Te , and right: ZnSe & ZnTe .

If the oxidation of the chalcogenide controls dissolution, then it may be expected that all sulfides should oxidise at the same rate. It has, however been shown that there is a correlation between the anodic dissolution charge (a measure of the dissolution rate) and the band gap of the sulfide or oxide.^{27, 29} This would seem logical as it defines the energy required to remove an electron from the conduction band. **Figure 7** shows the oxidative charge obtained from chronocoulometry experiments with copper chalcogenides plotted vs the direct band gap values. As the band gap increases and the material is more electrically resistive, the rate of dissolution decreases exponentially, i.e. an Arrhenius-type correlation, as would reasonably be expected. However, there is no direct correlation within the series with respect to chalcogenide type or oxidation state of the metal component showing that process kinetics are controlled by the band structure of the chalcogenide.

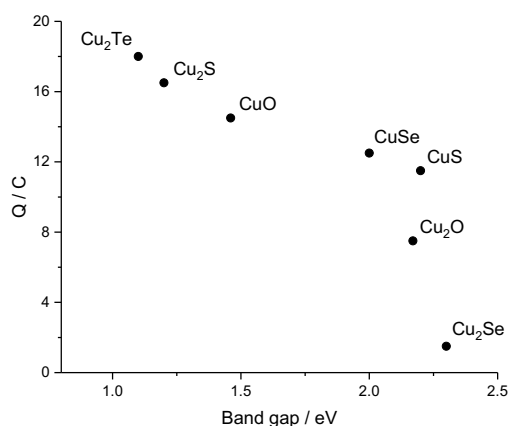


Figure 7. Graph of total charge passed during chronocoulometry vs literature direct band gap data.⁴⁷⁻⁵² Chronocoulometry was carried out at a constant potential of 1.2 V for 1800 s.

Conclusions

This study has shown that a wide variety of metal chalcogenides can be solubilised through electrochemical oxidation of the solid which has been cast as a paste on an electrode using a deep eutectic solvent. It was shown that all metal compounds dissolved through the oxidation of the chalcogenide. The redox chemistry of the chalcogenide appears to be similar to that observed in aqueous solutions with the chalcogenide forming oxo-complexes of the +IV and +VI oxidation state through reaction with traces of oxygen and/or water. All of the metals studied were released into solution as halide complexes of the form $[MCl_2]^-$ or $[MCl_4]^{x-}$. This is important as it shows that the chalcogenide is not associated with the metal when it dissolves. The oxo-chalcogenide complexes formed do not appear to be electroactive at the pH and over the potential range studied, hence the metal can be electrodeposited in a pure form without contamination from the chalcogenide. Although recovery of the chalcogenide from the solution was not a major part of this study, it was shown that for selenium and tellurium that this could be recovered using standard aqueous chemical methods. The rate of metal chalcogenide dissolution was shown to be related to the band gap of the material.

Conflicts of interest

There are no conflicts of interest to declare.

Acknowledgements

The authors would like to thank the NERC Minerals Security of Supply (SoS) grant NE/M010848/1 Tellurium and Selenium Cycling and Supply (TeaSe) and the Faraday Institution (Faraday Institution grant codes FIRG005 and FIRG006) for funding (project website <https://relib.org.uk>). This research also received funding from the European Commission's H2020 – Marie Skłodowska Curie Actions (MSCA) – Innovative Training Networks within the SOCRATES project under the grant agreement no. 721385 (project website: <http://etn-socrates.eu>), and from the Ministry of Education of Saudi Arabia and the Saudi Cultural Bureau (Grant number KAU1526).

Supporting Information

A figure showing the voltammetry of the grey substance deposited at the counter electrode during dissolution of PbSe, and a table of the chemicals used. This Supporting Information is accessible online.

References

1. Schuyler Anderson, C. *Mineral Commodity Summaries - Tellurium*; USGS: 2019; pp 166-167.
2. Schuyler Anderson, C. *Mineral Commodity Summaries - Selenium*; USGS: 2019; pp 146-147.
3. Bouroushian, M., *Electrochemistry of Metal Chalcogenides*. Springer-Verlag Berlin Heidelberg, 2010. DOI: 10.1007/978-3-642-03967-6

4. Wang, S., Tellurium, its resourcefulness and recovery. *JOM* **2011**, 63 (8), 90-93. DOI: 10.1007/s11837-011-0146-7
5. Ludvigsson, B. M.; Larsson, S. R., Anode slimes treatment: The boliden experience. *JOM* **2003**, 55 (4), 41-44. DOI: 10.1007/s11837-003-0087-x
6. Klemettinen, L.; Avarmaa, K.; Sukhomlinov, D.; O'Brien, H.; Taskinen, P.; Jokilaakso, A., Recycling of tellurium via copper smelting processes. *SN Applied Sciences* **2020**, 2 (3), 337. DOI: 10.1007/s42452-020-2137-1
7. Marwede, M.; Berger, W.; Schlummer, M.; Mäurer, A.; Reller, A., Recycling paths for thin-film chalcogenide photovoltaic waste – Current feasible processes. *Renew. Energy* **2013**, 55, 220-229. DOI: 10.1016/j.renene.2012.12.038
8. Smith, D. J.; Jenkin, G. R. T.; Holwell, D. A.; Kieth, M. In *Challenges and Opportunities in Tellurium Supply*, Proceedings of the 15th SGA Biennial Meeting, Glasgow, Scotland, 27-30 August 2019; pp 1654-1656.
9. Padoan, F. C. S. M.; Altimari, P.; Pagnanelli, F., Recycling of end of life photovoltaic panels: A chemical prospective on process development. *Sol. Energy* **2019**, 177, 746-761. DOI: 10.1016/j.solener.2018.12.003
10. Zhang, X.; Jiao, S.; Tu, J.; Song, W.-L.; Xiao, X.; Li, S.; Wang, M.; Lei, H.; Tian, D.; Chen, H.; Fang, D., Rechargeable ultrahigh-capacity tellurium–aluminum batteries. *Energy Environ. Sci.* **2019**, 12 (6), 1918-1927. DOI: 10.1039/c9ee00862d
11. Li, H.; Wang, K.; Zhou, H.; Guo, X.; Cheng, S.; Jiang, K., Tellurium-tin based electrodes enabling liquid metal batteries for high specific energy storage applications. *Energy Storage Mater.* **2018**, 14, 267-271. DOI: 10.1016/j.ensm.2018.04.017
12. Lu, D.-k.; Chang, Y.-f.; Yang, H.-y.; Xie, F., Sequential removal of selenium and tellurium from copper anode slime with high nickel content. *Trans. Nonferrous Met. Soc. China* **2015**, 25 (4), 1307-1314. DOI: 10.1016/s1003-6326(15)63729-3

13. Wang, W. K.; Hoh, Y.-C.; Chuang, W.-S.; Shaw, I.-S. Hydrometallurgical process for recovering precious metals from anode slime. U.S. Patent 4,293,332, 1981.
14. Smith, E. L.; Abbott, A. P.; Ryder, K. S., Deep eutectic solvents (DESs) and their applications. *Chem. Rev.* **2014**, *114* (21), 11060-82. DOI: 10.1021/cr300162p
15. Abbott, A. P.; Frisch, G.; Hartley, J.; Ryder, K. S., Processing of metals and metal oxides using ionic liquids. *Green Chem.* **2011**, *13* (3), 471-481. DOI: 10.1039/c0gc00716a
16. Binnemans, K.; Jones, P. T., Solvometallurgy: An Emerging Branch of Extractive Metallurgy. *J. Sus. Met.* **2017**, *3* (3), 570-600. DOI: 10.1007/s40831-017-0128-2
17. Jones, D.; Hartley, J.; Frisch, G.; Purnell, M.; Darras, L., Non-destructive, safe removal of conductive metal coatings from fossils: a new solution. *Palaeontologia Electronica* **2012**, *15.2.4T*, 1-7.
18. Jenkin, G. R. T.; Al-Bassam, A. Z. M.; Harris, R. C.; Abbott, A. P.; Smith, D. J.; Holwell, D. A.; Chapman, R. J.; Stanley, C. J., The application of deep eutectic solvent ionic liquids for environmentally-friendly dissolution and recovery of precious metals. *Miner. Eng.* **2016**, *87*, 18-24. DOI: 10.1016/j.mineng.2015.09.026
19. Saji, V. S.; Lee, C.-W., Selenium electrochemistry. *RSC Adv.* **2013**, *3* (26), 10058-10077. DOI: 10.1039/c3ra40678d
20. Agapescu, C.; Cojocaru, A.; Cotarta, A.; Visan, T., Electrodeposition of bismuth, tellurium, and bismuth telluride thin films from choline chloride–oxalic acid ionic liquid. *J. Appl. Electrochem.* **2012**, *43* (3), 309-321. DOI: 10.1007/s10800-012-0487-0
21. Golgovici, F.; Visan, T., Electrochemical deposition of BiTe films from choline chloride – malonic acid mixture as ionic liquid. *Chalcogenide Lett.* **2012**, *9* (10), 427-434.

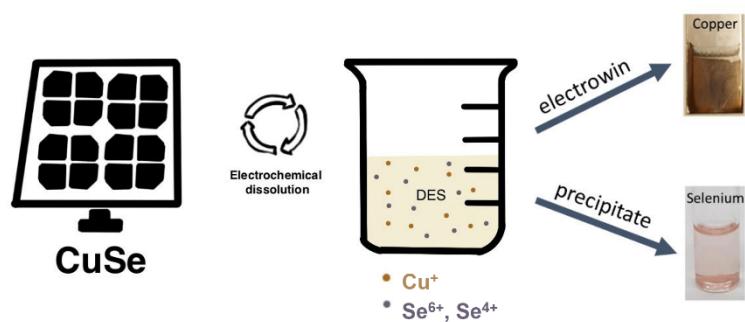
22. Anicai, L.; Sin, I.; Brincoveanu, O.; Costovici, S.; Cotarta, A.; Cojocaru, A.; Enachescu, M.; Visan, T., Electrodeposition of lead selenide films from ionic liquids based on choline chloride. *Appl. Surf. Sci.* **2019**, *475*, 803-812. DOI: 10.1016/j.apsusc.2018.12.191
23. Golgovici, F.; Visan, T., Cathodic deposition of components in PbTe compounds using choline chloride-ethylene glycol ionic liquids. *Chalcogenide Lett.* **2011**, *8* (8), 487-497.
24. Golgovici, F.; Catrangu, A.-S.; Visan, T., The Formation and Characterization of Copper Telluride Films from Choline Chloride – Urea Ionic Liquid. *Int. J. Electrochem. Sci.* **2016**, *11*, 915-928.
25. Catrangu, A. S.; Beregoi, M.; Cojocaru, A.; Anicai, L.; Cotarta, A.; Visan, T., Electrochemical deposition of zinc telluride thin films from Ethaline ionic liquid. *Chalcogenide Lett.* **2016**, *13* (5), 187-199.
26. Anggara, S.; Bevan, F.; Harris, R. C.; Hartley, J. M.; Frisch, G.; Jenkin, G. R. T.; Abbott, A. P., Direct extraction of copper from copper sulfide minerals using deep eutectic solvents. *Green Chem.* **2019**, *21* (23), 6502-6512. DOI: 10.1039/c9gc03213d
27. Hartley, J. M.; Al-Bassam, A. Z. M.; Harris, R. C.; Frisch, G.; Jenkin, G. R. T.; Abbott, A. P., Investigating the dissolution of iron sulfide and arsenide minerals in deep eutectic solvents. *Hydrometallurgy* **2020**, *198*. DOI: 10.1016/j.hydromet.2020.105511
28. Abbott, A. P.; Bevan, F.; Baeuerle, M.; Harris, R. C.; Jenkin, G. R. T., Paint casting: A facile method of studying mineral electrochemistry. *Electrochem. Commun.* **2017**, *76*, 20-23. DOI: 10.1016/j.elecom.2017.01.002
29. Pateli, I. M.; Abbott, A. P.; Jenkin, G. R. T.; Hartley, J. M., Electrochemical oxidation as alternative for dissolution of metal oxides in deep eutectic solvents. *Green Chem.* **2020**, *22* (23), 8360-8368. DOI: 10.1039/d0gc03491f

30. Abbott, A. P.; Frisch, G.; Gurman, S. J.; Hillman, A. R.; Hartley, J.; Holyoak, F.; Ryder, K. S., Ionometallurgy: designer redox properties for metal processing. *ChemComm* **2011**, 47 (36), 10031-3. DOI: 10.1039/c1cc13616j
31. Abbott, A. P.; Capper, G.; Davies, D. L.; Rasheed, R. K.; Tambyrajah, V., Novel solvent properties of choline chloride/urea mixtures. *ChemComm.* **2003**, 38 (1), 70-71. DOI: 10.1039/b210714g
32. Abbott, A. P.; Boothby, D.; Capper, G.; Davies, D. L.; Rasheed, R. K., Deep Eutectic Solvents Formed between Choline Chloride and Carboxylic Acids: Versatile Alternatives to Ionic Liquids. *J. Am. Chem. Soc.* **2004**, 126 (29), 9142-9147. DOI: 10.1021/ja048266j
33. Frenzel, N.; Hartley, J.; Frisch, G., Voltammetric and spectroscopic study of ferrocene and hexacyanoferrate and the suitability of their redox couples as internal standards in ionic liquids. *Phys. Chem. Chem. Phys.* **2017**, 19 (42), 28841-28852. DOI: 10.1039/c7cp05483a
34. Katayama, Y.; Fukui, R.; Miura, T., Electrodeposition of Lead from 1-butyl-1-methylpyrrolidinium Bis(trifluoromethylsulfonyl)amide Ionic Liquid. *J. Electrochem. Soc.* **2013**, 160 (6), D251-D255. DOI: 10.1149/2.112306jes
35. Liao, Y.-S.; Chen, P.-Y.; Sun, I. W., Electrochemical study and recovery of Pb using 1:2 choline chloride/urea deep eutectic solvent: A variety of Pb species $PbSO_4$, PbO_2 , and PbO exhibits the analogous thermodynamic behavior. *Electrochim. Acta* **2016**, 214, 265-275. DOI: 10.1016/j.electacta.2016.08.053
36. Gardner, J. R.; Woods, R., A study of the surface oxidation of galena using cyclic voltammetry. *J. Electroanal. Chem.* **1979**, 100 (1-2), 447-459. DOI: 10.1016/s0022-0728(79)80177-1

37. Dutrizac, J. E., The leaching of sulphide minerals in chloride media. *Hydrometallurgy* **1992**, 29 (1-3), 1-45. DOI: 10.1016/0304-386x(92)90004-j
38. Martínez-Gómez, V. J.; Fuentes-Aceituno, J. C.; Pérez-Garibay, R.; Lee, J.-c., A study of the electro-assisted reductive leaching of a chalcopyrite concentrate in HCl solutions. Part I: Kinetic behavior and nature of the chalcopyrite reduction. *Hydrometallurgy* **2018**, 181, 195–205. DOI: 10.1149/1.1509459
39. Lu, Z. Y.; Jeffrey, M. I.; Lawson, F., An electrochemical study of the effect of chloride ions on the dissolution of chalcopyrite in acidic solutions. *Hydrometallurgy* **2000**, 56 (2), 145-155. DOI: 10.1016/s0304-386x(00)00068-2
40. Pourbaix, M., *Atlas of Electrochemical Equilibria in Aqueous Solutions*. NACE International & Celebcor: Houston, Texas, USA & Brussels, 1974.
41. Tsai, R.-W.; Hsieh, Y.-T.; Chen, P.-Y.; Sun, I. W., Voltammetric study and electrodeposition of tellurium, lead, and lead telluride in room-temperature ionic liquid 1-ethyl-3-methylimidazolium tetrafluoroborate. *Electrochim. Acta* **2014**, 137, 49-56. DOI: 10.1016/j.electacta.2014.05.099
42. Rudnik, E.; Biskup, P., Electrochemical Studies of Lead Telluride Behavior in Acidic Nitrate Solutions. *Arch. Metall. Mater.* **2015**, 60 (1), 95-100. DOI: 10.1515/amm-2015-0015
43. Hartley, J. M.; Ip, C. M.; Forrest, G. C.; Singh, K.; Gurman, S. J.; Ryder, K. S.; Abbott, A. P.; Frisch, G., EXAFS study into the speciation of metal salts dissolved in ionic liquids and deep eutectic solvents. *Inorg. Chem.* **2014**, 53 (12), 6280-6288. DOI: 10.1021/ic500824r
44. Abbott, A. P.; Alabdullah, S. S. M.; Al-Murshedi, A. Y. M.; Ryder, K. S., Bronsted acidity in deep eutectic solvents and ionic liquids. *Faraday Discuss.* **2018**, 206, 365-377. DOI: 10.1039/c7fd00153c

45. Bevan, F. Electrochemical Processing of Metal Chalcogenides in Deep Eutectic Solvents. PhD thesis, University of Leicester, 2019.
46. Feigl, F.; Anger, V., Tests for the Elements, their Ions and Compounds. In *Spot Tests in Inorganic Analysis*, 1972; pp 94-524. DOI: 10.1016/b978-0-444-40929-4.50007-5
47. Jagminas, A.; Juškėnas, R.; Gailiūtė, I.; Statkutė, G.; Tomašiūnas, R., Electrochemical synthesis and optical characterization of copper selenide nanowire arrays within the alumina pores. *J. Cryst. Growth* **2006**, *294* (2), 343-348. DOI: 10.1016/j.jcrysgro.2006.06.013
48. Montes-Monsalve, J. I.; Correa, R. B.; Mora, A. P., Optical and Structural Study of CuSe and CuSe/In Thin Films. *J. Phys. Conf. Ser.* **2014**, *480*. DOI: 10.1088/1742-6596/480/1/012024
49. Wang, Y.; Lany, S.; Ghanbaja, J.; Fagot-Revurat, Y.; Chen, Y. P.; Soldera, F.; Horwat, D.; Mücklich, F.; Pierson, J. F., Electronic structures of Cu₂O, Cu₄O₃, and CuO: A joint experimental and theoretical study. *Phys. Rev. B* **2016**, *94* (24), 245418. DOI: 10.1103/PhysRevB.94.245418
50. Chaki, S. H.; Deshpande, M. P.; Tailor, J. P., Characterization of CuS nanocrystalline thin films synthesized by chemical bath deposition and dip coating techniques. *Thin Solid Films* **2014**, *550*, 291-297. DOI: 10.1016/j.tsf.2013.11.037
51. Ramya, M.; Ganesan, S., Study of thickness dependent characteristics of Cu₂S thin film for various applications. *Iran. J. Mater. Sci. Eng.* **2011**, *8* (2), 34-40.
52. Hameed, T. A.; Moustafa, S. H.; Shaban, H.; Mansour, B. A., The effect of selenium on the structural, morphology, optical, electrical properties of Cu₂Te thin films for thermoelectric and photovoltaic applications. *Opt. Mater.* **2020**, *109*. DOI: 10.1016/j.optmat.2020.110308

For Table of Contents Use Only



Metal chalcogenide compounds can be anodically dissolved in deep eutectic solvents and selectively separated via electrowinning and precipitation

A unified method for the recovery of metals from chalcogenides

Francesca Bevan,^a Hanaa Galeb,^{a,b} Alexander Black,^a Ioanna Maria Pateli,^{a,c} Jack Allen,^a

Magali Perez,^d Jörg Feldmann,^{d,e} Robert Harris,^a Gawen Jenkin,^f Andrew Abbott,^a

Jennifer Hartley^{a}*

^a School of Chemistry, University of Leicester, University Road, Leicester, LE1 7RH, UK

^b Department of Chemistry, King Abdulaziz University, 21577 Jeddah, Saudi Arabia

^c Stephenson Institute for Renewable Energy, University of Liverpool, Peach Street, Liverpool, L69 7ZF, UK

^d Department of Chemistry, University of Aberdeen, Meston Walk, Aberdeen, AB24 3UE, UK

^e Institute of Chemistry, University of Graz, Universitätsplatz 1/I, 8010 Graz, Austria

^f School of Geography, Geology and the Environment, University of Leicester, University Road, Leicester, LE1 7RH, UK

Number of pages: 3

Number of figures: 1

Number of tables: 1

Supporting information

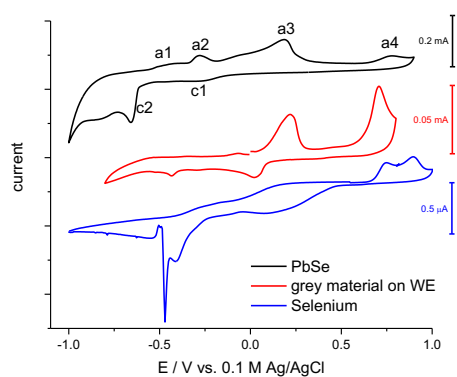


Figure S1. Voltammogram of grey material present on the working electrode after repeated cycling of PbSe, compared to the voltammograms of paint casted PbSe and elemental selenium (left), and an image of this grey coating (right).

Table S1. Chemicals and purities used in the present work.

Chemical	Purity / %	Source
Bismuth chloride (BiCl ₃)	<98	Aldrich
Bismuth selenide (Bi ₂ Se ₃)	≥99.995	Sigma Aldrich
Bismuth telluride (Bi ₂ Te ₃)	99.99	Sigma Aldrich
Copper(I) chloride (CuCl)	≥99	Sigma Aldrich
Copper(II) chloride (CuCl ₂)	99	Acros Organics
Copper(I) oxide (Cu ₂ O)	99.9	Alfa Aesar
Copper(I) sulfide (Cu ₂ S)	99.5	Alfa Aesar
Copper(I) selenide (Cu ₂ Se)	99.95	Sigma Aldrich
Copper(I) telluride (Cu ₂ Te)	99.5	Alfa Aesar
Lead(II) chloride (PbCl ₂)	98	Aldrich
Lead(II) oxide (PbO)	99.999	Alfa Aesar
Lead(II) sulfide (PbS)	99.9	Aldrich
Lead(II) selenide (PbSe)	99.999+	Alfa Aesar
Lead(II) telluride (PbTe)	99.99	Alfa Aesar
Silver chloride (AgCl)	99.9	Alfa Aesar
Silver sulfide (Ag ₂ S)	n.a.	Chem Cruz
Silver selenide (Ag ₂ Se)	n.a.	Aldrich
Silver telluride (Ag ₂ Te)	n.a.	Aldrich
Sodium sulfide nonahydrate (Na ₂ S)	≥98	Honeywell
Sodium selenide (Na ₂ Se)	99.8	Alfa Aesar
Sodium selenite (Na ₂ SeO ₃)	99	Sigma Aldrich
Sodium selenate (Na ₂ SeO ₄)	99.8+	Alfa Aesar
Sodium telluride (Na ₂ Te)	99.9	Alfa Aesar
Sodium tellurite (Na ₂ TeO ₃)	99	Alfa Aesar
Sodium tellurate (Na ₂ TeO ₄)	99	Sigma Aldrich
Zinc chloride (ZnCl ₂)	>98	Sigma Aldrich
Zinc sulfide (ZnS)	99.99	Aldrich
Zinc selenide (ZnSe)	99.99	Alfa Aesar
Zinc telluride (ZnTe)	99.99	Alfa Aesar